Derivation of Numerical Lifting Line from Phillips and Snyder

Cory D. Goates *
Utah State University, Logan, Utah, 84322

Nomenclature

α	=	angle of attack
c	=	chord length
$\bar{c}$	=	mean aerodynamic chord length
C	=	aerodynamic coefficient
d	=	differential element
δ	=	flap deflection
ε	=	flap efficiency
$\boldsymbol{F}$	=	aerodynamic force vector
G	=	dimensionless vortex strength
Γ	=	vortex strength
l	=	length
L	=	lift force
N	=	number of horseshoe vortices/control points
r	=	position
$\boldsymbol{R}$	=	residual vector
ρ	=	density
s	=	spanwise position
S	=	planform area
$\boldsymbol{u}$	=	directional unit vector
v	=	dimensionless velocity
V	=	velocity
x	=	x-coordinate
y	=	y-coordinate
z	=	z-coordinate
ζ	=	dimensionless length

*Graduate Intern, Autonomy & Navigation Technology, Air Force Institute of Technology

Subscripts

a	=	axial direction
i	=	control point/horseshoe vortex index
ind	=	induced
∞	=	freestream
j	=	horseshoe vortex index
$L0$	=	zero-lift state
n	=	normal direction
r	=	global reference
s	=	spanwise direction
,	=	derivative with respect to
0	=	inbound horseshoe vortex node
1	=	outbound horseshoe vortex node

Superscripts

$\tilde{}$	=	section property

(Note: Boldface variables indicate vector quantities. Plain text variables indicate a vector magnitude or scalar quantity. Boldface variables in brackets indicate a matrix.)

I. Introduction

The purpose of this document is to present the derivation of a modified version of Prandtl's lifting-line theory developed by Phillips and Snyder [1]. This modified version is referred to as numerical lifting-line. This derivation of numerical lifting-line is taken from Phillips [2]. The author assumes the reader already has an understanding of the derivation and working of Prandtl's classic lifting-line theory. We will first discuss some of the weaknesses of Prandtl's classic lifting-line theory and how these are addressed by numerical lifting-line. We will then derive numerical lifting-line theory, both the full nonlinear equation and a linearized version.

II. Classic Lifting Line

Prandtl's classic lifting-line theory has long been the most widely-used and efficient theory for design of finite lifting surfaces. It is able to accurately model the inviscid lift, drag, and moments produced by lifting surfaces with reasonably large aspect ratios. However, it has some weaknesses. First, Prandtl's theory can only be applied to lifing surfaces with no sweep or dihedral. If one looks at modern aircraft, it is easy to see how limited this is, as almost all modern aircraft incorporate some amount of sweep or dihedral.

The other major weakness to Prandtl's classic lifting-line theory is that it can only be applied to a single lifting surface, such as a wing in free flight. Research and testing have shown that the flow field created by a lifting surface has a significant impact on the performance of the other lifting surfaces on an aircraft. By iteratively applying Prandtl's theory to each lifting surface in turn, taking into account the flow fields already determined, this effect can be approximated, but this approach is expensive and has limited accuracy.

Prandtl's theory also assumes the trailing vortex segments are aligned with the wing section chord line. This allows an analytical solution to be obtained but is not representative of reality. This assumption limits the accuracy of Prandtl's theory.

III. Numerical Lifting Line

In numerical lifting line, the flow around a finite lifting surface is modelled by a set of horseshoe vortices. Each vortex consists of three segments, a finite segment that is bound to the quarter-chord of the lifting surface and two semi-infinite segments which extend from each end of the bound segment to the fluid boundary at infinity. The bound segments are distributed along the locus of section aerodynamic centers for the lifting surface such that they cover the entire span but to not overlap.

As shown in Fig. 1, the trailing vortex segments are aligned with the freestream and form a vortex sheet. Fig. 1 shows a slight gap between the trailing vortex segments of neighboring horseshoe vortices. This is only done to show that two vortices are shed from each interior point; in reality, the shed vortex segments are coincident.

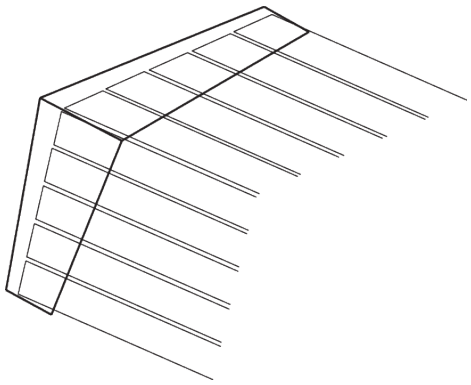

Fig. 1 Distribution of horseshoe vortices along the locus of aerodynamic centers of a swept lifting surface [3].

In deriving numerical lifting line, we make no assumptions about the bound vortex segments forming a straight line, and so the lifting surface can take any shape. This also allows for multiple lifting surfaces to be modeled at once with interactions between lifting surfaces being accounted for. A wing-tail combination can be modeled using numerical lifting line with great accuracy. Having the trailing vortices aligned with the freestream also leads to greater accuracy than Prandtl's theory.

IV. Derivation of Numerical Lifting Line

A. Assumptions

Numerical lifting line is derived from potential flow and so all assumptions from potential flow (inviscid, incompressible, etc.) hold for numerical lifting line as well. We assume the bound segment of each horseshoe vortex lies along the locus of wing section aerodynamic centers for its associated lifting surface. We also assume the trailing vortex segments are aligned with the freestream.

B. Distribution of Horseshoe Vortices

We begin by selecting a distribution of nodes along the locus of aerodynamic centers of each lifting surface, beginning and ending at the wingtips (see Fig. 1). Each pair of adjacent nodes, referred to as (x_0, y_0, z_0) and (x_1, y_1, z_1), along with the direction of the freestream velocity and a vortex strength, fully define a horseshoe vortex. As shown in Fig. 2, a horseshoe vortex consists of a single finite, bound segment and two semi-infinite, trailing segments. The bound segment of the vortex extends between the two nodes. One trailing segment extends from the head of the bound vortex segment to the fluid boundary at infinity. The other trailing segment extends from the fluid boundary to the tail of the bound segment. Both trailing segments are parallel to the freestream velocity.

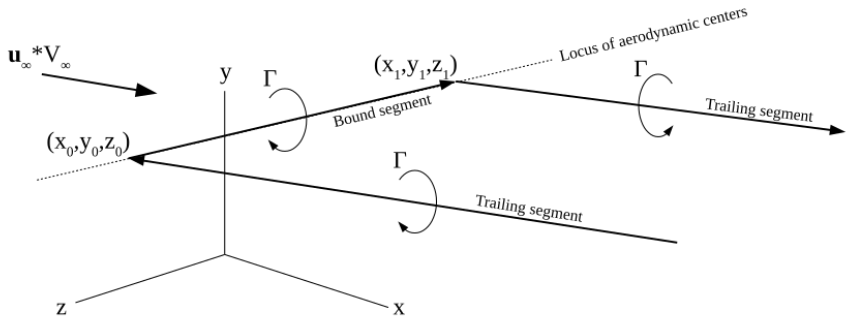

Fig. 2 Schematic of a single horseshoe vortex showing nodes, bound segment, trailing segments, and circulation.

From potential flow, it can be shown that the velocity vector induced at any given point (x, y, z) by a straight vortex segment is given by:

$$\boldsymbol{V_{ind}} = \frac{\Gamma}{4\pi} \frac{(r_0 + r_1)(\boldsymbol{r_0} \times \boldsymbol{r_1})}{r_0 r_1 (r_0 r_1 + \boldsymbol{r_0} \cdot \boldsymbol{r_1})} \tag{1}$$

And the velocity vector induced at any given point (x, y, z) by a straight, semi-infinite vortex segment is given by:

$$\boldsymbol{V_{ind}} = \frac{\Gamma}{4\pi} \frac{\boldsymbol{u_\infty} \times \boldsymbol{r_0}}{r_0 (r_0 - \boldsymbol{u_\infty} \cdot \boldsymbol{r_0})} \tag{2}$$

Where $\boldsymbol{r_0}$ and $\boldsymbol{r_1}$ are given by:

$$\boldsymbol{r_0} = (x - x_0)\boldsymbol{i_x} + (y - y_0)\boldsymbol{i_y} + (z - z_0)\boldsymbol{i_z} \tag{3}$$

$$\boldsymbol{r_1} = (x - x_1)\boldsymbol{i_x} + (y - y_1)\boldsymbol{i_y} + (z - z_1)\boldsymbol{i_z} \tag{4}$$

Note that in the formulation of Eq. (2), the vortex segment being considered is assumed to start at $\boldsymbol{r_0}$ and extend to the fluid boundary. To apply this to the inbound trailing vortex, the circulation is assumed to be opposite what it really is. The velocity induced at any point in the flow by a single horseshoe vortex is then the vector sum of the velocities induced by each segment:

$$\boldsymbol{V_{ind}} = \frac{\Gamma}{4\pi}\left(-\frac{\boldsymbol{u_\infty} \times \boldsymbol{r_0}}{r_0(r_0 - \boldsymbol{u_\infty} \cdot \boldsymbol{r_0})} + \frac{(r_0 + r_1)(\boldsymbol{r_0} \times \boldsymbol{r_1})}{r_0 r_1(r_0 r_1 + \boldsymbol{r_0} \cdot \boldsymbol{r_1})} + \frac{\boldsymbol{u_\infty} \times \boldsymbol{r_1}}{r_1(r_1 - \boldsymbol{u_\infty} \cdot \boldsymbol{r_1})}\right) \tag{5}$$

For numerical lifting-line, we synthesize a flow field from a freestream and a set of horseshoe vortices. We can then define the local velocity at any control point placed on the bound segment of a given vortex as:

$$\boldsymbol{V_{ind}} = \boldsymbol{V_\infty} + \sum_{j=1}^{N} \frac{\Gamma_j \boldsymbol{v_{ji}}}{\bar{c}_j} \tag{6}$$

Where $\boldsymbol{v_{ji}}$ is the dimensionless velocity induced at control point i by horseshoe vortex j, assuming horseshoe vortex j has a unit strength. This velocity is given by Eq. (7).

$$\boldsymbol{v_{ji}} = \begin{cases} \frac{\bar{c}_j}{4\pi}\left(-\frac{\boldsymbol{u_\infty} \times \boldsymbol{r_{j_0 i}}}{r_{j_0 i}(r_{j_0 i} - \boldsymbol{u_\infty} \cdot \boldsymbol{r_{j_0 i}})} + \frac{(r_{j_0 i} + r_{j_1 i})(\boldsymbol{r_{j_0 i}} \times \boldsymbol{r_{j_1 i}})}{r_{j_0 i} r_{j_1 i}(r_{j_0 i} r_{j_1 i} + \boldsymbol{r_{j_0 i}} \cdot \boldsymbol{r_{j_1 i}})} + \frac{\boldsymbol{u_\infty} \times \boldsymbol{r_{j_1 i}}}{r_{j_1 i}(r_{j_1 i} - \boldsymbol{u_\infty} \cdot \boldsymbol{r_{j_1 i}})}\right), & j \neq i \\ \frac{\bar{c}_j}{4\pi}\left(-\frac{\boldsymbol{u_\infty} \times \boldsymbol{r_{j_0 i}}}{r_{j_0 i}(r_{j_0 i} - \boldsymbol{u_\infty} \cdot \boldsymbol{r_{j_0 i}})} + \frac{\boldsymbol{u_\infty} \times \boldsymbol{r_{j_1 i}}}{r_{j_1 i}(r_{j_1 i} - \boldsymbol{u_\infty} \cdot \boldsymbol{r_{j_1 i}})}\right), & j = i \end{cases} \tag{7}$$

The formula is different when $j = i$ because the bound segment of a horseshoe vortex does not induce velocity on its own control point.

C. Vortex Lifting Law

The Kutta-Joukowski law states that the lift produced by a two-dimensional body is directly proportional to the circulation it produces. In three dimensions, this is presented as the vortex lifting law. This law states the force per unit length exerted by a vortex filament in a freestream is given by:

$$\boldsymbol{dF} = \rho \Gamma \boldsymbol{V} \times \boldsymbol{dl} \tag{8}$$

Using Eq. (6) in Eq. (8), we obtain Eq. (9), which gives the force per unit length generated by the bound vortex segment of a given horseshoe vortex i.

$$\boldsymbol{dF_i} = \rho\Gamma_i \left(\boldsymbol{V_\infty} + \sum_{j=1}^{N} \frac{\Gamma_j \boldsymbol{v_{ji}}}{c_j} \right) \times \boldsymbol{dl_i} \tag{9}$$

Where:

$$\boldsymbol{dl_i} = (x_{1i} - x_{0i})\boldsymbol{i_x} + (y_{1i} - y_{0i})\boldsymbol{i_y} + (z_{1i} - z_{0i})\boldsymbol{i_z} \tag{10}$$

The total aerodynamic force generated by the lifting surfaces can be found by integrating force per unit length across the length of each bound vortex and then summing these forces. However, the strength of each vortex is still unknown. We determine the strength of each vortex from a knowledge of airfoil section parameters as a function of angle of attack.

D. Airfoil Section Parameters

For any given control point, the section lift coefficient can be determined as a function of angle of attack and flap deflection:

$$\widetilde{C}_{Li} = \widetilde{C}_{Li}(\alpha_i, \delta_i) \tag{11}$$

Where α_i is given by:

$$\alpha_i = \arctan\left(\frac{\boldsymbol{V_i} \cdot \boldsymbol{u_{ni}}}{\boldsymbol{V_i} \cdot \boldsymbol{u_{ai}}} \right) \tag{12}$$

Where $\boldsymbol{u_{ni}}$ and $\boldsymbol{u_{ai}}$ are the section unit normal and axial vectors, respectively.

Since the only aerodynamic force produced by an airfoil section in potential flow is lift, the magnitude of section aerodynamic force at each control point given by Eq. (9) must be equal to the section lift. Dimensionalizing Eq. (11) gives:

$$|\boldsymbol{dF_i}| = \frac{1}{2}\rho V_i^2 \widetilde{C}_{Li}(\alpha_i, \delta) dS_i \tag{13}$$

E. Full Nonlinear Numerical Lifting-Line

For any given control point along the lifting surface, the aerodynamic force predicted by Eqs. (9) and (13) must be the same, or:

$$\left| \rho\Gamma_i \left(\boldsymbol{V_\infty} + \sum_{j=1}^{N} \frac{\Gamma_j \boldsymbol{v_{ji}}}{c_j} \right) \times \boldsymbol{dl} \right| - \frac{1}{2}\rho V_i^2 \widetilde{C}_{Li}(\alpha_i, \delta_i) dS_i = 0 \tag{14}$$

Simplifying, Eq. (14) can be written as:

$$2\left|\left(\boldsymbol{u}_\infty + \sum_{j=1}^{N} G_j \boldsymbol{v_{ji}}\right) \times \boldsymbol{\zeta_i}\right| G_i - \widetilde{C}_{Li}(\alpha_i, \delta) = 0 \tag{15}$$

Where:

$$\boldsymbol{u}_\infty \equiv \frac{\boldsymbol{V}_\infty}{V_\infty} \tag{16}$$

$$\boldsymbol{\zeta_i} \equiv c_i \frac{\boldsymbol{dl_i}}{dS_i} \tag{17}$$

$$G_i \equiv \frac{\Gamma_i}{c_i V_\infty} \tag{18}$$

$$\alpha_i = \arctan\left(\frac{\left(\boldsymbol{u}_\infty + \sum_{j=1}^{N} G_j \boldsymbol{v_{ji}}\right) \cdot \boldsymbol{u_{ni}}}{\left(\boldsymbol{u}_\infty + \sum_{j=1}^{N} G_j \boldsymbol{v_{ji}}\right) \cdot \boldsymbol{u_{ai}}}\right) \tag{19}$$

Equation (15) is the governing equation of numerical lifting-line. When evaluated at N control points (one attached to the bound segment of each horseshoe vortex), Eq. (15) becomes a nonlinear system of N equations. There are N unknowns, namely, the dimensionless strength of each horseshoe vortex. If these strengths are written as a vector, $\boldsymbol{G}$, the whole system can then be written as a vector:

$$f(\boldsymbol{G}) = \boldsymbol{R} \tag{20}$$

Where:

$$f_i(\boldsymbol{G}) = 2\left|\left(\boldsymbol{u}_\infty + \sum_{j=1}^{N} G_j \boldsymbol{v_{ji}}\right) \times \boldsymbol{\zeta_i}\right| G_i - \widetilde{C}_{Li}(\alpha_i, \delta) \tag{21}$$

F. Solution Method

The system represented by Eq. (20) can be readily solved using Newton's method. Using an initial guess for $\boldsymbol{G}$, we come up with an initial value for $\boldsymbol{R}$. We then want to update $\boldsymbol{G}$ until all elements of $\boldsymbol{R}$ go to 0. We do this using Newton's corrector formula:

$$[\boldsymbol{J}]\Delta\boldsymbol{G} = -\boldsymbol{R} \tag{22}$$

Where the Jacobian, $[\boldsymbol{J}]$, is a matrix of partial derivatives. This matrix is obtained by differentiating every element of f with respect to every element of $\boldsymbol{G}$:

$$J_{ij} = \frac{\partial}{\partial G_j}\left(2\left|\left(\boldsymbol{u_\infty} + \sum_{j=1}^{N} G_j \boldsymbol{v_{ji}}\right) \times \boldsymbol{\zeta_i}\right| G_i - \widetilde{C}_{Li}(\alpha_i, \delta)\right) \tag{23}$$

To evaluate the second term in the right half of Eq. (23), we use the chain rule:

$$\frac{\partial \widetilde{C}_{Li}}{\partial G_j} = \frac{\partial \widetilde{C}_{Li}}{\partial \alpha_i}\frac{\partial}{\partial G_j}\left(\arctan\left(\frac{\left(\boldsymbol{u_\infty} + \sum_{j=1}^{N} G_j \boldsymbol{v_{ji}}\right) \cdot \boldsymbol{u_{ni}}}{\left(\boldsymbol{u_\infty} + \sum_{j=1}^{N} G_j \boldsymbol{v_{ji}}\right) \cdot \boldsymbol{u_{ai}}}\right)\right) \tag{24}$$

Evaluating the derivative yields:

$$\frac{\partial \widetilde{C}_{Li}}{\partial G_j} = \frac{\partial \widetilde{C}_{Li}}{\partial \alpha_i}\left(1 + \left[\frac{\left(\boldsymbol{u_\infty} + \sum_{j=1}^{N} G_j \boldsymbol{v_{ji}}\right) \cdot \boldsymbol{u_{ni}}}{\left(\boldsymbol{u_\infty} + \sum_{j=1}^{N} G_j \boldsymbol{v_{ji}}\right) \cdot \boldsymbol{u_{ai}}}\right]^2\right)^{-1}\left[\frac{\left(\left(\boldsymbol{u_\infty} + \sum_{j=1}^{N} G_j \boldsymbol{v_{ji}}\right) \cdot \boldsymbol{u_{ai}}\right)(\boldsymbol{v_{ji}} \cdot \boldsymbol{u_{ni}}) - \left(\left(\boldsymbol{u_\infty} + \sum_{j=1}^{N} G_j \boldsymbol{v_{ji}}\right) \cdot \boldsymbol{u_{ni}}\right)(\boldsymbol{v_{ji}} \cdot \boldsymbol{u_{ai}})}{\left(\left(\boldsymbol{u_\infty} + \sum_{j=1}^{N} G_j \boldsymbol{v_{ji}}\right) \cdot \boldsymbol{u_{ai}}\right)^2}\right] \tag{25}$$

The derivative of the first term in the right half of Eq. (23) depends upon whether $j = i$. For the case where $j = i$, we must use the product rule:

$$\frac{\partial}{\partial G_j}\left(2\left|\left(\boldsymbol{u_\infty} + \sum_{j=1}^{N} G_j \boldsymbol{v_{ji}}\right) \times \boldsymbol{\zeta_i}\right| G_i\right) = 2\left|\left(\boldsymbol{u_\infty} + \sum_{j=1}^{N} G_j \boldsymbol{v_{ji}}\right) \times \boldsymbol{\zeta_i}\right| + 2G_i \frac{\partial}{\partial G_j}\left(\sqrt{\left(\left(\boldsymbol{u_\infty} + \sum_{j=1}^{N} G_j \boldsymbol{v_{ji}}\right) \times \boldsymbol{\zeta_i}\right) \cdot \left(\left(\boldsymbol{u_\infty} + \sum_{j=1}^{N} G_j \boldsymbol{v_{ji}}\right) \times \boldsymbol{\zeta_i}\right)}\right) \tag{26}$$

Evaluating the derivative, Eq. (26) yields:

$$2\left|\left(\boldsymbol{u_\infty} + \sum_{j=1}^{N} G_j \boldsymbol{v_{ji}}\right) \times \boldsymbol{\zeta_i}\right| + \frac{2G_i}{\left|\left(\boldsymbol{u_\infty} + \sum_{j=1}^{N} G_j \boldsymbol{v_{ji}}\right) \times \boldsymbol{\zeta_i}\right|}\left(\left(\boldsymbol{u_\infty} + \sum_{j=1}^{N} G_j \boldsymbol{v_{ji}}\right) \times \boldsymbol{\zeta_i}\right) \cdot (\boldsymbol{v_{ji}} \times \boldsymbol{\zeta_i}) \tag{27}$$

For the case where $j \neq i$, the product rule is no longer needed and the first term of Eq. (27) disappears, yielding:

$$\frac{2G_i}{\left|\left(\boldsymbol{u_\infty} + \sum_{j=1}^{N} G_j \boldsymbol{v_{ji}}\right) \times \boldsymbol{\zeta_i}\right|}\left(\left(\boldsymbol{u_\infty} + \sum_{j=1}^{N} G_j \boldsymbol{v_{ji}}\right) \times \boldsymbol{\zeta_i}\right) \cdot (\boldsymbol{v_{ji}} \times \boldsymbol{\zeta_i}) \tag{28}$$

For the sake of conciseness, we apply the following substitutions to the above derivatives:

$$\boldsymbol{v_i} \equiv \boldsymbol{u_\infty} + \sum_{j=1}^{N} G_j \boldsymbol{v_{ji}} \tag{29}$$

$$\boldsymbol{w_i} \equiv \boldsymbol{v_i} \times \boldsymbol{\zeta_i} \tag{30}$$

$$v_{ni} \equiv \boldsymbol{v_i} \cdot \boldsymbol{u_{ni}} \tag{31}$$

$$v_{ai} \equiv \boldsymbol{v_i} \cdot \boldsymbol{u_{ai}} \tag{32}$$

Applying the above substitutions and simplifying, we obtain the final solution for each element of $[\boldsymbol{J}]$:

$$J_{ij} = \begin{cases} \frac{2G_j \boldsymbol{w_i}(\boldsymbol{v_{ji}} \times \boldsymbol{\zeta})}{|\boldsymbol{w_i}|} - \frac{\partial \widetilde{C}_{Li}}{\partial \alpha_i} \left[\frac{v_{ai}(\boldsymbol{v_{ji}} \cdot \boldsymbol{u_{ni}}) - v_{ni}(\boldsymbol{v_{ji}} \cdot \boldsymbol{u_{ai}}}{v_{ai}^2 + v_{ni}^2} \right], & j \neq i \\ 2|\boldsymbol{w_i}| + \frac{2G_j \boldsymbol{w_i}(\boldsymbol{v_{ji}} \times \boldsymbol{\zeta})}{|\boldsymbol{w_i}|} - \frac{\partial \widetilde{C}_{Li}}{\partial \alpha_i} \left[\frac{v_{ai}(\boldsymbol{v_{ji}} \cdot \boldsymbol{u_{ni}}) - v_{ni}(\boldsymbol{v_{ji}} \cdot \boldsymbol{u_{ai}}}{v_{ai}^2 + v_{ni}^2} \right], & j = i \end{cases} \tag{33}$$

Using this formulation for $[\boldsymbol{J}]$, we can solve Eq. (22) for $\Delta \boldsymbol{G}$. We then update $\boldsymbol{G}$ using:

$$\boldsymbol{G_{k+1}} = \boldsymbol{G_k} + \psi \Delta \boldsymbol{G} \tag{34}$$

Where ψ is a relaxation factor (typically unity). We continue iterating until the vector of residuals, $\boldsymbol{R}$, falls below some specified threshold.

G. Determination of Forces and Moments

Once the distribution of vortex strengths is known, we can sum Eq. (9) across all vortices to find the total aerodynamic force and moment for each lifting surface. The total aerodynamic force is given by:

$$\boldsymbol{F} = \rho \sum_{i=1}^{N} \Gamma_i \left(\boldsymbol{V_\infty} + \sum_{j=1}^{N} \frac{\Gamma_j \boldsymbol{v_{ji}}}{c_j} \right) \times \boldsymbol{dl_i} \tag{35}$$

Non-dimensionalizing this result, we obtain:

$$\frac{\boldsymbol{F}}{\frac{1}{2}\rho V_\infty^2 S_r} = \sum_{i=1}^{N} G_i \left(\boldsymbol{u_\infty} + \sum_{j=1}^{N} G_j \boldsymbol{v_{ji}} \right) \times \boldsymbol{\zeta_i} \frac{dS_i}{S_r} \tag{36}$$

Similarly, the total aerodynamic moment is given by:

$$\boldsymbol{M} = \rho \sum_{i=1}^{N} \left[\boldsymbol{r_i} \times \left[\Gamma_i \left(\boldsymbol{V_\infty} + \sum_{j=1}^{N} \frac{\Gamma_j \boldsymbol{v_{ji}}}{c_j} \right) \times \boldsymbol{dl_i} \right] - \frac{1}{2} V_\infty^2 \widetilde{C}_{mi} \int_{s=s_1}^{s_2} c^2 ds \boldsymbol{u_{si}} \right] \tag{37}$$

Where:

$$\boldsymbol{u_{si}} = \boldsymbol{u_{ai}} \times \boldsymbol{u_{ni}} \tag{38}$$

Non-dimensionalizing this result, we obtain:

$$\frac{\boldsymbol{M}}{\frac{1}{2}\rho V_\infty^2 S_r l_r} = \sum_{i=1}^{N} \left[2\boldsymbol{r_i} \times \left[G_i \left(\boldsymbol{u_\infty} + \sum_{j=1}^{N} \frac{G_j \boldsymbol{v_{ji}}}{c_j} \right) \times \boldsymbol{\zeta_i} \right] - \frac{\widetilde{C}_{mi}}{dS_i} \int_{s=s_1}^{s_2} c^2 ds \boldsymbol{u_{si}} \right] \frac{dS_i}{S_r l_r} \tag{39}$$

H. Linearized Governing Equation

For Newton's method to quickly converge to the solution vector of vortex strengths, an accurate starting estimate is required. This can be done by linearizing Eq. (15) and using matrix inversion to solve for $\boldsymbol{G}$. Assuming a linear lift slope, the right half of Eq. (15) can be written as:

$$\widetilde{C}_{Li}(\alpha_i, \delta_i) \approx \widetilde{C}_{Li,\alpha}(\alpha_i - \alpha_{L0_i} + \varepsilon_i \delta_i) \tag{40}$$

Where α_i is given by Eq. (19). Assuming small angles, the local velocity will be almost parallel to the axial vector. This makes the denominator in Eq. (19) become unity. Assuming small angles, the arctan in Eq. (19) can also be dropped. Eq. (40) can then be written as:

$$\widetilde{C}_{Li}(\alpha_i, \delta_i) \approx \widetilde{C}_{Li,\alpha} \left(\left(\boldsymbol{u_\infty} + \sum_{j=1}^{N} G_j \boldsymbol{v_{ji}} \right) \cdot \boldsymbol{u_{ni}} - \alpha_{L0_i} + \varepsilon_i \delta_i \right) \tag{41}$$

Neglecting second-order terms, the right half of Eq. (15) can be written as:

$$2 \left| \boldsymbol{u_\infty} \times \boldsymbol{\zeta_i} \right| G_i \tag{42}$$

Combining these equations and gathering all terms including $\boldsymbol{G}$ to the left-hand side, we obtain the linearized version of Eq. (15):

$$2 \left| \boldsymbol{u_\infty} \times \boldsymbol{\zeta_i} \right| G_i - \widetilde{C}_{Li,\alpha} \sum_{j=1}^{N} G_j \boldsymbol{v_{ji}} \cdot \boldsymbol{u_{ni}} = \widetilde{C}_{Li,\alpha} \left(\boldsymbol{u_\infty} \cdot \boldsymbol{u_{ni}} - \alpha_{L0_i} + \varepsilon_i \delta_i \right) \tag{43}$$

Equation (43) is readily solved using matrix inversion to provide an initial guess for solving Eq. (15). This estimate also proves remarkably accurate even as a final result for lifting surfaces with high aspect ratios and low angles of attack.

V. Conclusion

In this paper, we presented a modification to Prandtl's classic lifting-line theory called numerical lifting-line. Numerical lifting-line presents several advantages over classical lifting-line, the foremost being its ability to model swept lifting surfaces with dihedral as well as multiple lifting surfaces at once. We presented the assumptions numerical lifting-line is based upon and developed the equations governing the set of vortices used to model the lifting surfaces. Using a knowledge of airfoil section parameters, we derived the governing equation for finding the vector of vortex strengths. We also derived the Jacobian of the governing equation with respect to vortex strength to use in Newton's method for solving the governing equation. We then demonstrated how the vortex strengths can be summed to determine total aerodynamic forces and moments. We also derived a linearized version of the governing equation, which provides a good initial estimate for Newton's method.

References

[1] Phillips, W. F., and Snyder, D. O., "Modern Adaptation of Prandtl's Classic Lifting-Line Theory," *Journal of Aircraft*, Vol. 37, No. 4, 2000.

[2] Phillips, W. F., *Mechanics of Flight*, 2nd ed., John Wiley & Sons, Hoboken, New Jersey, 2010, Chap. 1.9.

[3] Hunsaker, D., "A Numerical Lifting-Line Method Using Horseshoe Vortex Sheets," 2011.